ELSEVIER

Earth and Planetary Science Letters 186 (2001) 297–309

EPSL

www.elsevier.com/locate/epsl

Bubble plumes generated during recharge of basaltic magma reservoirs

Jeremy C. Phillips [a], Andrew W. Woods [b,*]

[a] *Centre for Environmental and Geophysical Flows, School of Mathematics, University of Bristol, Bristol BS8 1TW, UK*
[b] *BP Institute for Multiphase Flow, Madingley Rise, Madingley Road, Cambridge CB3 0EZ, UK*

Received 17 August 2000; accepted 22 January 2001

Abstract

CO_2 is relatively insoluble in basaltic magma at low crustal pressures. It therefore exists as a gas phase in the form of bubbles in shallow crustal reservoirs. Over time these bubbles may separate gravitationally from the magma in the chamber. As a result, any new magma which recharges the chamber from deeper in the crust may be more bubble-rich and hence of lower density than the magma in the chamber. Using scaling arguments, we show that for typical recharge fluxes, such a source of low-viscosity, bubble-rich basalt may generate a turbulent bubble plume within the chamber. We also show that the bubbles are typically sufficiently small to have a low Reynolds number and to remain in the flow. We then present a series of analogue laboratory experiments which identify that the motion of such a turbulent bubble-driven line plume is well described by the classical theory of buoyant plumes. Using the classical plume theory we then examine the effect of the return flow associated with such bubble plumes on the mixing and redistribution of bubbles within the chamber. Using this model, we show that a relatively deep bubbly layer of magma may form below a thin foam layer at the roof. If, as an eruption proceeds, there is a continuing influx at the base of the chamber, then our model suggests that the bubble content of the bubbly layer may gradually increase. This may lead to a transition from lava flow activity to more explosive fire-fountaining activity. The foam layer at the top of the chamber may provide a flux for the continual outgassing from the flanks of the volcano [Ryan, Am. Geophys. Union Geophys. Monogr. 91 (1990)] and if it deepens sufficiently it may contribute to the eruptive activity [Vergniolle and Jaupart, J. Geophys. Res. 95 (1990) 2793–3001].

Keywords: volatiles; exsolution; bubbles; convection; buoyancy; plumes

1. Introduction

Geophysical surveys [3,4] and measurements of surface gas fluxes [1,5] suggest that basaltic magma is stored in shallow magma chambers, 2–4 km below the surface and of volume 0.1–10 km^3 prior to eruption or emplacement along lateral dikes. Owing to the low solubility of CO_2 at pressures associated with the shallow crust, these chambers contain a large number of exsolved CO_2 bubbles [1,6,7]. The vertical distribution of such bubbles can have a key impact on the style of eruption. Volatile-rich magma is likely to lead to violent fire-fountaining activity while volatile-poor magma may produce vesicular lava flows [6,8,9]. As well as the relatively short-lived eruption episodes

* Corresponding author. E-mail: aww1@hermes.cam.ac.uk

0012-821X/01/$ – see front matter
PII: S0012-821X(01)00221-7

of explosive and lava flow activity, surface measurements over several decades have established that there is continual degassing of CO_2 through the volcanic edifice [1,5]. Any vertical redistribution of bubbles within the chamber may therefore also have a key impact on the resulting style of eruptive activity. In fact, Woods and Cardoso [10] have shown that the vertical separation of bubbles from the magma may even elevate the pressure sufficiently to trigger an eruption.

Owing to the importance of the bubble transport and distribution within the chamber, the purpose of this study is to examine the flow generated in the chamber as it is recharged by a flux of bubbly magma. Our main interest is in establishing some understanding of the general fluid mechanical processes involved, rather than simulating a particular eruption. However, we do draw some general conclusions about the possible implications of our model for Hawaiian-style volcanism. As a conceptual model, it is assumed that a sill or shallow chamber is recharged by bubbly magma issuing from a dike [6,7]. The dike acts as a linear source at the base of the chamber. For large recharge rates and small bubbles, this flux may generate a coherent turbulent bubble plume while for smaller recharge rates, it may lead to the isolated ascent of individual bubbles through the liquid. Both of these scenarios can lead to a complex range of eruption phenomena, especially since the eruption dynamics depend on the conditions in the chamber as well as the flow in the overlying conduit.

Jaupart and Vergniolle [6,7] examined the recharge of the chamber by a source of large bubbles distributed over the base of the chamber. Through a series of analogue laboratory experiments and accompanying theoretical models, they showed that the bubbles may rise through the magma and pond to form a foam at the roof of the chamber, while little motion is generated in the magma itself. They developed a model for the evolution of this foam, accounting for both the recharge from below and eruption of the foam along a conduit to the surface. Two main types of activity may arise in such an open system. In the first, the foam becomes unstable and develops large slugs of gas which then ascend from the chamber along the conduit to the surface. Such activity is reminiscent of the discrete explosions observed at Stromboli-style vents. In the second, the foam remained stable, or exhibited limited coalescence, and the bubbly mixture ascended along the conduit to the surface, leading to fire-fountaining activity. Although this study identified a range of interesting possible flow regimes and eruption conditions, their experimental observations concerned relatively large bubbles which ascend individually through the magma. However, if the rise speed of the bubbles is sufficiently small then, instead of individual bubble ascent, coherent convection of the buoyant bubbly magma mixture may develop [11]. We now investigate the importance of such convection in the redistribution of bubbles through a basaltic chamber, focussing on the motions generated from localised line sources of bubbly magma, as would occur with magma supplied along a dike intersecting the sill or chamber. Such convection may retain a large number of bubbles in suspension. We also account for the observations of widespread gas release on the flanks of the volcanic edifice [1] by allowing gas to leak from the reservoir through the permeable host rock to the surface. Both of these processes conspire to reduce the deepening of the foam layer which tends to accumulate at the chamber roof and in some cases may lead to eruption of the bubbly magma rather than the overlying foam. First we present a series of scaling arguments to identify conditions under which bubble-driven convection rather than the isolated motion of individual bubbles will develop. We then describe a series of analogue laboratory experiments to investigate the properties of such bubble-driven plumes and we develop a quantitative model of the flow. Finally, we use this to model the evolution of a crustal basaltic magma chamber as it is recharged by a mixture of magma and bubbles. We consider both a closed and an open system.

2. Turbulent bubble plume flow regime

When a flux of bubbles is supplied to the base of a liquid layer, a range of flow regimes may

develop depending on the rise speed of the bubbles through the liquid, and the flux of bubbles supplied to the liquid. In order to determine the typical flow regime associated with a localised linear source of bubbles, we present some scaling relations in which we compare the speed of individual bubbles with the speed of bulk convective motions which may be generated by the bubbles.

We consider the case in which a dike of typical width 1–2 m and lateral extent $L \approx 100$–1000 m produces a localised line source of magma into the chamber. For a total volume flux recharging the chamber in the range 1–10 m^3/s [2,4], the flux per unit length of the dike is $Q \approx 0.001$–0.1 m^2/s. For a bubble volume flux Q_b and magma flux $Q_m = Q - Q_b$ per unit length, the fraction of this recharge composed of volatiles bubbles is $v = Q_b/Q$. In the absence of any two-phase flow effects deeper in the system, which may elevate the mass fraction of CO_2 in the magma, the volume fraction of exsolved CO_2 recharging the chamber is approximately:

$$v = n\rho_m/((1-n)\rho_g + n\rho_m) \approx n\rho_m/\rho_g \quad (1)$$

where n is the original CO_2 mass fraction in the basalt, which has values of order 1 wt% [8], and ρ_g and ρ_m are the gas and magma densities respectively. In writing Eq. 1 we assume that at shallow crustal pressures of order 10^8 Pa (2–4 km depth) only a small fraction of the CO_2 (≤ 0.1 wt%) remains in solution [12,13]. At such pressures, the density of the CO_2 bubbles may be approximated with the perfect gas law:

$$\rho_g = \frac{P}{RT} \quad (2)$$

where $R = 185$ J/kg/K, and the temperature $T \approx 1400$ K. The density of the bubbles is therefore typically of order 5–10 times smaller than that of the liquid magma, $\rho_m \approx 2600$ kg/m^3, so that $v \approx 10n$ and the gas flux recharging the chamber $Q_b \approx 0.0001$–0.01 m^2/s. The effective acceleration of gravity of these bubbles relative to the magma is known as the reduced gravity or buoyancy, and has value $g' = g(\rho_m - \rho_s)/\rho_m$. The flux of this reduced gravity or buoyancy is then given by:

$$B = Q_b g(\rho_m - \rho_g)/\rho_m \quad (3)$$

Using the above numbers, this flux has values in the range $B \approx 0.001$–0.1 m^3/s^3. Note that for simplicity we neglect the small fraction of H_2O which, owing to the the presence of exsolved CO_2, may also come out of solution even though the pressures associated with a magma reservoir are relatively large in the context of H_2O solubility [12].

If the Reynolds number, Re, of the resulting bubbly magma flow is sufficient to produce a turbulent plume, $Re \geq 10^3$, then we may use dimensional arguments to determine the bulk properties of the motion. In particular, the speed of a turbulent line plume scales as [14]:

$$u_t \approx 2B^{1/3} \quad (4)$$

Hence the Reynolds number for such a flow at height z above the source scales as:

$$Re = \rho u_t r(z)/\mu \approx 2\varepsilon\rho B^{1/3} z/\mu \quad (5)$$

where $r(z) \approx \varepsilon z$ is the plume width and we expect $\varepsilon \approx 0.25$ (see experiments below). The Reynolds number increases with height z above the actual source and as shown in Fig. 1, it has values in excess of 10^3 at heights of order 10 m above the source for low-viscosity Hawaiian basalt, $10 \leq \mu \leq 50$ Pa s (Fig. 1) [15]. We deduce that for low-viscosity Hawaiian magma, such bubble plumes may be turbulent.

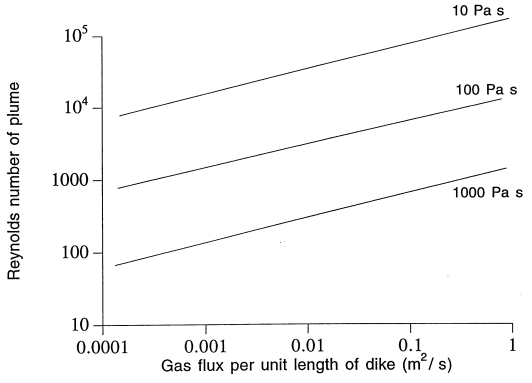

Fig. 1. The Reynolds number associated with a turbulent buoyant plume as a function of the source gas flux at a height of 10 m above the source. Curves are shown for magma of viscosity 10, 100 and 1000 Pa s. For $Re \geq 10^3$ the motion is fully turbulent and the model applies.

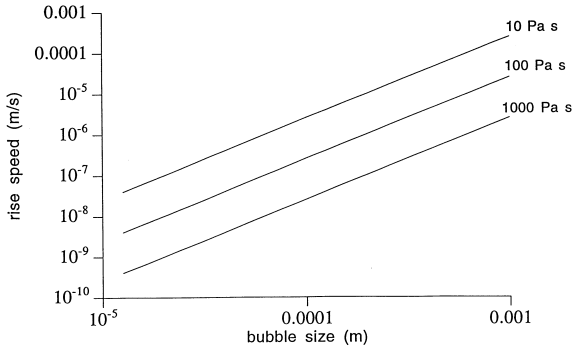

Fig. 2. The mean vertical speed in a turbulent buoyant plume as a function of the bubble size. Curves are given for magma of viscosity 10, 100 and 1000 Pa s.

The dynamics and structure of a two-phase bubble plume is in general complex and depends crucially on the rise speed of the bubbles relative to the bulk speed of the plume [16,17]. Although the exact sizes of the bubbles in basaltic chambers are not known, surface observations of vesicular pumice suggest that they may be of order 0.01–1.0 mm [2,18–21], and so rise according to Stokes' law [22,23] with rise speed:

$$v_s \approx \frac{g(\rho_m - \rho_g)d^2}{3\mu} \qquad (6)$$

where d is the bubble diameter. The upward speed of the turbulent plume has values in the range $0.1 \leq u_t \leq 1$ m/s according to Eq. 4. As seen in Fig. 2, the bubble rise speed is several orders of magnitude smaller than this. We deduce that the recharge flux of magma and CO_2 bubbles can generate a turbulent bubble plume within the chamber, and that in such a plume, the effects of liquid–bubble slip may be negligible.

If the Reynolds number falls below a value of order 10^3, for example in more viscous magma ($\mu \geq 100$ Pa s) or with smaller recharge fluxes, ($Q \leq 0.01$ m^3/s) then the motion will not become fully turbulent and the entrainment flux will decrease, and eventually it becomes very small; however, here we focus on the high flux limit.

3. Analogue experiments

The dynamics of turbulent buoyant plumes driven by thermal or solutal anomalies is well understood [14,24], and models of the bulk motion have been tested experimentally to constrain the rate of entrainment and the return flows induced in the ambient fluid in a confined geometry. We expect the motion of a turbulent bubble plume composed of bubbles with very small velocity relative to the plume velocity to be similar; however, we are not aware of any experimental measurements of such bubble plumes. Experi-

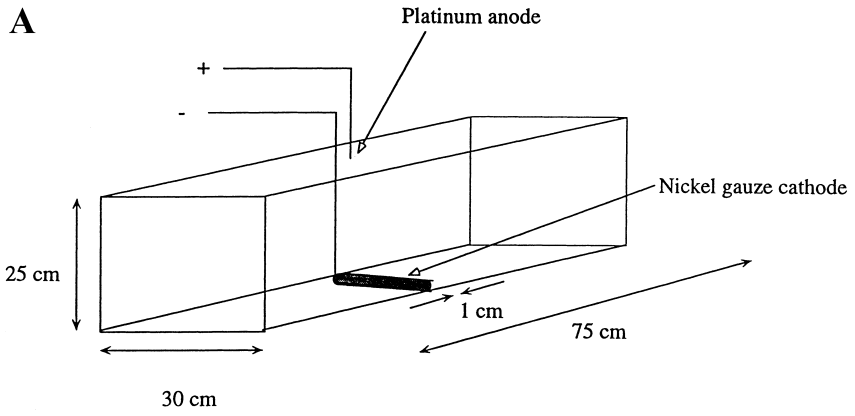

Fig. 3. (A) Schematic of the experimental apparatus. (B) Sequence of photographs showing the development of the turbulent bubble plume and the return flow in the experimental tank. The upper 1 cm of the fluid in the tank was dyed red to enable visualisation of the return flow. The bubble plume is viewed along axis in these photographs, and appears anomalously white relative to the surrounding fluid.

Fig. 3 (*continued*).

ments on bubble plumes have largely considered plumes driven by rapidly rising bubbles in which two-phase flow effects are important [16,17]. We have therefore conducted an experimental study of bubble plumes driven by relatively small bubbles.

An electrolysis cell was set up in a glass tank $75 \times 30 \times 25$ cm containing 2 wt% saline solution,

using a 1 cm wide strip of 20 mesh nickel gauze with wire diameter 180 μm as the cathode and a platinum wire as the anode. The nickel gauze was positioned centrally across the tank base, with the platinum wire immersed just below the free surface (Fig. 3A). A 12 V power supply was used to drive the electrolysis cell, which produced bubbles with diameters 20–50 μm [25] at the nickel gauze. This formed a turbulent line plume at an applied current of 0.8 A (Fig. 3B). The bulk velocity of the plume was of order 0.1–1.0 cm/s and was therefore in excess of the individual rise speed of the bubbles, 0.001–0.01 cm/s. The bubble flux produced by this equipment was subsequently measured by installing the anode and cathode in a smaller tank which was sealed except for a 1 mm diameter tube. The gas flux produced by the electrolysis drove a liquid film up this tube enabling its direct measurement [26].

A series of experiments was conducted to determine the rate of entrainment of ambient fluid into the plume by measuring the return flow in the ambient fluid (Fig. 3B) [27]. This return flow has an important influence on the distribution of bubbles in the reservoir. The return flow is readily measured by following the position $z_d(t)$ of a dyed surface in the tank as a function of time t. By conservation of mass, the downward volume flux in a large tank of length L equals the net upward flow in the plume:

$$L\frac{dz_d}{dt} \approx -Q(z_d) \tag{7}$$

where L is the width of the chamber in the cross-source direction, $Q(z)$ is the flux in the plume at height z, per unit distance along the source.

Plume theory [14,24] suggests that the volume flux varies with height through entrainment according to:

$$Q(z) = \lambda B^{1/3}(z + z_o) \tag{8}$$

where z_o is the position of the virtual origin of the plume behind the actual source and λ depends on the rate of entrainment and may be determined by experiment [14,24,28]. In the present experiments, the location of the real source ahead of the virtual origin, z_o, was estimated from the plume shape to be of order $z_o \approx 2 \pm 0.2$ cm. Combining Eqs. 7 and 8 leads to the prediction that the position of the dye surface in the ambient fluid $z_d(t)$ decreases with time according to:

$$z_d(t) = (H + z_o >)\exp\left(-\frac{\lambda B^{1/3}}{L}(t - t_o)\right) - z_o \tag{9}$$

where H is the depth of the fluid and at the initial time, $t = t_o$ we set $z_d(0) = H$.

In order to determine whether the bubble plume satisfies the entrainment law (Eq. 8), we have plotted the experimental measurements of the descending interface in the form $\ln(z_d(t)+z_o)$ as a function of t (Fig. 4). Comparison of the data with the model identifies some differences particularly at early and late times in the experiment. Differences at long times arise as the filling box front approaches the region just above the source of the plume, where the entrainment may not be fully established in the plume (List, 1980) and this leads to a reduction in the speed of the filling front, as observed for $t > 600$ s. Differences at short times may be associated with the time required for the initial intrusion of fluid to spread out at the top of the reservoir, before the return flow becomes fully established. However, during the main part of the experiment the data do appear to follow a straight line. This suggests that the model entrainment law (Eq. 8) provides a rea-

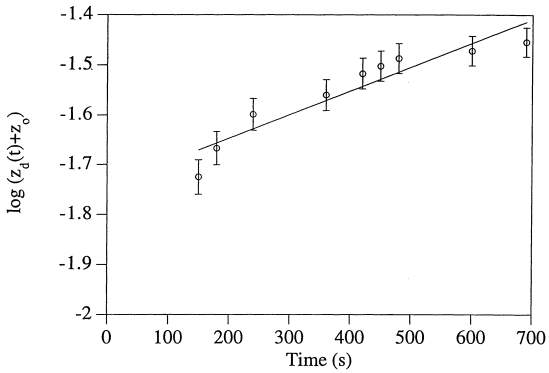

Fig. 4. Experimental measurements of the position of the filling front as a function of time. In the figure, we show $\log(z_d(t)+z_o)$ as a function of time. Using the calibrated buoyancy flux, the best fit line to the data suggests that the entrainment parameter $\lambda = 0.37$.

sonable leading order description of the flow. Measurement of the bubble flux produced by the gauze suggests that the buoyancy flux per unit length associated with the line plume has value 5×10^{-10} m^3/s^3. The slope of the straight line in Fig. 4 has value $\sim4\pm1\times10^{-4}$ s^{-1}, where the error bar reflects the uncertainty in the duration of the early and long time transient flows. According to plume theory this should equal $\lambda B^{1/3}/L$, and so we estimate that $\lambda\approx0.37\pm0.1$. This is consistent with measurements of saline plane plumes for which $\lambda\approx0.34$ as reported by List [28], suggesting that the horizontally averaged properties of a turbulent small bubble-driven line plume may be described using a similar model to that for the classical single-phase turbulent line plume.

The return flow in the ambient fluid has an important effect on the distribution of bubbles in the ambient fluid. As a simple model, we would expect the bubbles to be advected downwards in the tank up to the point at which the rise speed of the bubbles equals the downward return flow. Below this level, the rise speed will exceed the return flow speed. In order to test this model for the depth of the bubbly layer, we conducted a series of experiments in which the total depth of the fluid layer was varied from 15 to 30 cm, while the plume had the same source flux of bubbles. In each experiment, the system was allowed to evolve to steady state, with an upper bubble-rich layer overlying a bubble-free layer of fluid. According to plume theory, the bubble-free layer should be independent of the overall depth of the fluid since the upward flux in the plume and hence return flow only depend on the distance from the source. As a result, the bubble-rich layer should deepen with the depth of the fluid layer. In Fig. 5 we present experimental measurements of the depth of the bubble-free layer as a function of the overall depth of fluid. Data are presented for three experimental tanks, with areas 625 cm^2, 1328 cm^2 and 2250 cm^2. To good approximation, in the two smaller tanks, the depth of the bubble-free zone is independent of the layer depth. In the largest tank, the effect of gravitational bubble separation from the horizontally intruding flow at the top of the plume becomes more important

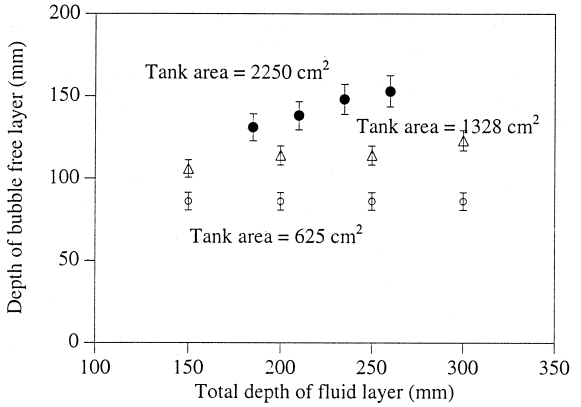

Fig. 5. Experimental measurements of the depth of the bubble-free layer as a function of the depth of the liquid layer. As predicted by the theory, the depth of the bubble-free layer is independent of the overall fluid depth.

as the time for the intrusion to spread to the far boundary of the tank increases. This modifies the uniformity of the downward return flow, since the bubble content in the horizontal intrusion far from the plume may be much less than that near the plume; as a result, the recirculation flow is not uniform, and is not as efficient in transporting bubbles downwards, in contrast to the classical filling box process of Baines and Turner [27]. The volume flux delivered to the top of the plume scales as $Q\approx B^{1/3}H$, the time to spread to the end of the tank scales as $\tau_e\approx L/u$, and the time for bubbles to rise through this horizontal flow is $\tau_b\approx h/v_s$. The ratio of these time scales $\tau_e/\tau_b\approx Lv_s/hu\approx Lv_s/B^{1/3}H$. The return flow will only be uniform if $\tau_e\ll\tau_b$, and so in a sufficiently large reservoir, $L\geq B^{1/3}H/v_s$, the horizontally averaged model for the return flow will break down. However, this effect may not be relevant in the magmatic context; indeed, for fluxes of order 10 m^2/s at the plume top, and for a chamber of width 1 km and with bubbles with rise speed 10^{-5} m/s, the ratio of time scales, τ_e/τ_b, is about 10^{-3}. Therefore, in a geological context, we expect that the flow will reach the end of the tank long before any bubble separation occurs, and the classical filling box model for a buoyant turbulent plume should apply, and we do not expect two-phase flow effects in the plume to be important [16].

4. Implications for basaltic eruptions

The scaling arguments of Section 2 suggest that as shallow basaltic sills are replenished with a bubble–magma mixture, a turbulent bubble plume may develop. This generates a large-scale flow in the chamber which may have an important effect on the bubble distribution within the chamber (Fig. 6) so that the original volatile composition in the magma may be very different from that in the eruption products. It is therefore of interest to study the time scales associated with the different processes in order to determine whether, prior to eruption, the bubbles may be effectively redistributed throughout the magma as a result of the formation of a bubble plume. This is an important consideration since the volatile/bubble distribution within the chamber can have an important impact on the style of eruption [2]. Volatile-rich magmas are likely to produce fire-fountaining activity while more degassed magma will lead to effusive bubbly lava flows [8,9].

In order to develop some general principles, we consider the two idealised end-member models of a closed and open magma reservoir. For the closed reservoir, we assume the pre-existing magma is bubble-poor and we examine how the volatile content evolves during the recharge. We assume that the recharge leads to a gradual inflation of the chamber until a critical overpressure is attained when the surrounding rock fails and allows magma to erupt at the surface. For the open system, we assume that the gas and magma erupt as the chamber is recharging. We also allow for the possibility that some of the gas can escape through fractures in the chamber roof and then through the permeable overlying country rock [29].

4.1. Closed system

4.1.1. Time for pressure build-up

The continuing flux of magma and bubbles into the system leads to a gradual increase in the chamber pressure. As a simple model, we can assume that the chamber walls expand elastically, until reaching a critical overpressure of order 10^7 Pa, comparable to the strength of rock, at which point the walls fail and eruption ensues [12]. Bower and Woods [30] have shown that at

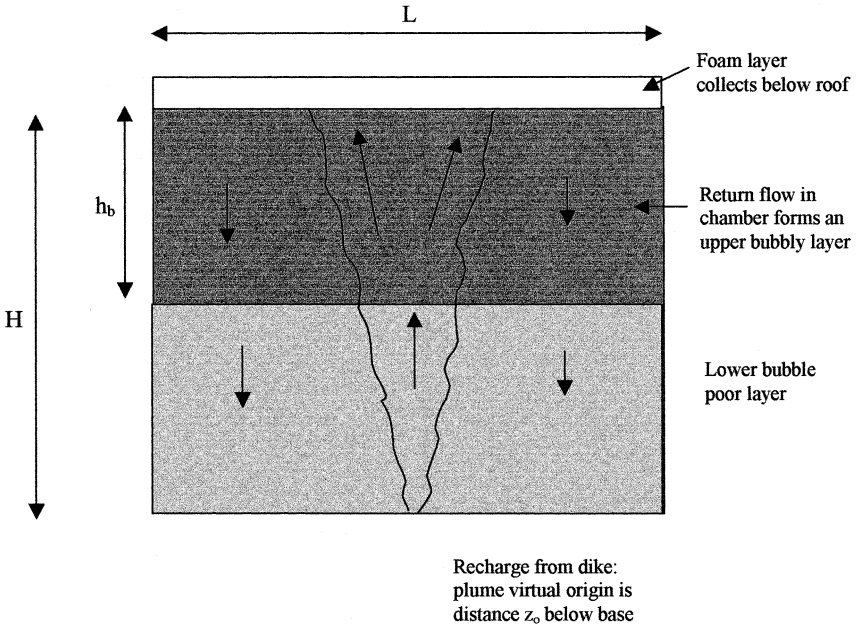

Fig. 6. Schematic of the mixing and bubble redistribution in a magma chamber produced by the turbulent line plume.

pressures of 10^8 Pa, volatile–magma mixtures with a CO_2 volatile fraction of order 1 wt% have a bulk modulus value of order 10^9–10^{10} Pa, and so we estimate that the fractional increase in volume of the chamber necessary to trigger eruption is of order 10^{-2}–10^{-3}. For a chamber of volume 1–10 km^3, and recharge rate of 1–10 m^3/s, this requires 10^5–10^8 s.

4.1.2. The return flow time scale

Prior to the eruption, the bubble plume supplies a low-concentration magma–bubble mixture to the top of the chamber where it spreads out and forms a bubbly layer at the chamber top. The return flow in the interior of the chamber, which is driven by the entrainment, draws down this bubbly plume fluid, which then deepens from the top of the chamber (Fig. 6). However, even if there is unlimited time, the bubbles may only be drawn down to form a layer of depth h_b above the floor at which the downward speed equals the rise speed of the bubbles (Section 3). This is expressed by the relation (cf. Eq. 7):

$$\lambda B^{1/3}(H-h_b+z_o)/L = v_s \qquad (10)$$

where L is the width of the chamber in the cross-dike direction, v_s is given by Eq. 6 and z_o is the depth of the virtual origin below the point at which the dike intersects the chamber (cf. Section 3). This is typically of order 1 m for $Q \approx 0.001$–0.1 m^2/s. It is interesting to note that the depth of the bubble-poor layer, $H-h_b$, is independent of the depth of the chamber, since it only depends on the upward flux in the plume at that level, the width of the chamber and the bubble rise speed (cf. Fig. 5). In Fig. 7 we show how the depth of this lower bubble-poor layer scales with the gas recharge flux and the rise speed of the bubbles. In the parameter range of interest for basaltic systems, this layer is extremely thin, of order 1–10 m, so that once steady state has been attained, we expect the main body of magma in the chamber to be bubble-rich.

The time required for the first front, associated with the downward return flow, to reach this level may be found from the equation for the conservation of mass, Eq. 9 [27]:

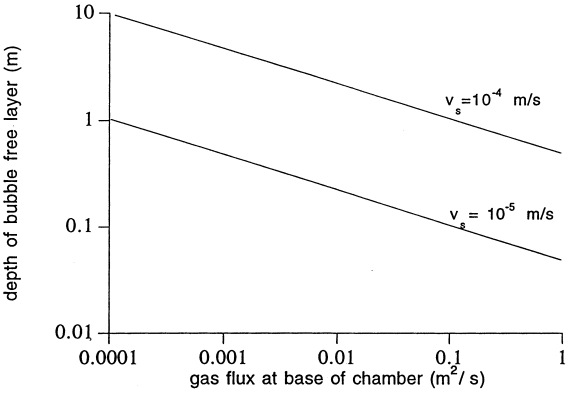

Fig. 7. Calculation of the equilibrium depth of the bubble-free layer at the base of the chamber as a function of the gas flux at the base of the chamber. Curves are shown for chambers of cross-dike width 1.0 km, and bubble rise speed of 10^{-5} m/s and 10^{-4} m/s.

$$L\frac{dz}{dt} = -\lambda B^{1/3}(z+z_o) \qquad (11)$$

Using Eq. 10 in the solution of Eq. 11 identifies that the time for the first front to reach the point $z = H-h_b$ is given by:

$$\tau = \frac{L}{\lambda B^{1/3}}\ln\left(\frac{(H+z_o)\lambda B^{1/3}}{Lv_s}\right) \qquad (12)$$

For a typical buoyancy flux 10^{-3} m^3/s, in a chamber of width $L \approx 1$–10 km, this front requires 10^4–10^6 s to pass this point. However, since the rise speed of the bubbles becomes comparable to the speed of the first front near $z = h_b$, the bubbly layer grows more slowly. A simple expression for the rate of deepening of the bubbly layer, $h(t)$, may be obtained by adding the rise speed of the bubbles, v_s, with the return flow:

$$\frac{dh}{dt} = \frac{\lambda B^{1/3}}{L}(H-h+z_o)-v_s \qquad (13)$$

which identifies that the time τ required for the bubbly layer to attain depth $h < h_b$ is:

$$\tau \approx \frac{L}{\lambda B^{1/3}}\ln\left(\frac{h_b}{h_b-h}\right) \qquad (14)$$

For example, for a typical buoyancy flux 10^{-3} m^3/s, in a chamber of width $L \approx 1$–10 km, the time scale for half of the bubble layer to become

established $(L/\lambda B^{1/3})\ln(2) \approx 10^5$–$10^6$ s. Since this time is shorter than or comparable to the time until eruption, we deduce from Fig. 7 that at the point of eruption, the bubbly layer will constitute a significant fraction of the chamber depth. Being the upper layer, it is likely that at the onset of eruption this bubbly layer will erupt. The style of eruption depends on the volatile content; we now explore how this depends on the input flux as well as the loss of bubbles at the top of the layer.

4.1.3. The upper foam layer

In the laboratory experiments, as the bubbly layer forms, and the bubble concentration increases, the bubbles tend to rise against the downflow, driving bubbly convection and producing a well-mixed layer, in a similar fashion to that described by Cardoso and Woods [11]. The rate of loss of bubbles from this layer, per unit length, then depends on the concentration, c, the rise speed of the bubbles, v_s, and the width of the chamber according to the law [11,31]:

$$F_b = -Lv_s c \tag{15}$$

Assuming that the layer becomes well-mixed, then the concentration of bubbles, $c(t)$, in this layer of depth $h(t)$ evolves according to the balance between the flux supplied by the plume, Q_b, and the loss, F_b, so that:

$$L\frac{\mathrm{d}hc}{\mathrm{d}t} = Q_b + F_b \tag{16}$$

If we couple the equation for the deepening of the bubbly layer (Eq. 13) with this bubble conservation relation (Eq. 16), we obtain the expression for the evolution of the bubble concentration:

$$Lh_b[1-\exp(-\lambda B^{1/3}t/L]\frac{\mathrm{d}c}{\mathrm{d}t} =$$

$$Q_b - Lv_s c[1 + (\lambda B^{1/3}h_b/Lv_s)\times\exp(-\lambda B^{1/3}t/L)] \tag{17}$$

where $H^* = H - v_s L/\lambda B^{1/3}$ and $F = \lambda B^{1/3}/L \approx 10^{-5}$. Fig. 8 shows the increase in bubble concentration c of the bubbly zone as a function of time for a recharge gas flux of 0.001 m^2/s in chambers of

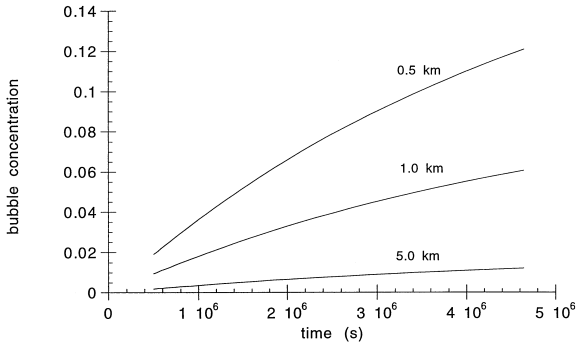

Fig. 8. Calculation of the variation in concentration of the bubbly layer in a 500 m deep chamber as a function of time, for chambers of cross-dike width 0.5, 1.0 and 5.0 km for a source of magma and bubbles with buoyancy flux 10^{-3} m^3/s^3.

width $L = 5000$, 1000 and 500 m and depth 500 m, and with a bubble rise speed, $v_s = 10^{-5}$ m/s. For comparison, the eruption time, based on the time for pressure build-up in the chamber, $\tau_e \approx (10^{-2}$–$10^{-3})HL/Q$, has values of order 2×10^5–2×10^7 s, with the larger values corresponding to the larger chambers. We deduce that, at the point of eruption, the bubbly layer may occupy a significant part of the chamber (Eq. 14) although the concentration of the bubbly layer may be considerably smaller than the steady value. Owing to the low concentration, there is only a small flux of bubbles to the upper foam layer from the bubbly layer (Fig. 6) before the eruption occurs. Depending on the precise strength of the country rock and the compressibility of the bubble–magma mixture at the point of eruption, the additional bubble volume fraction associated with the recharge may only be of order 0.01–0.05, corresponding to a mass fraction of about 0.2–1.0 wt%. Our results suggest that, in some situations with magma of low volatile content, the eruption may initially involve bubbly lava effusion. However, as the system evolves and the bubble content rises then the style of activity may also evolve into more explosive activity.

4.2. Open system

If the magmatic system is open to the atmosphere, or a surface lava lake, then there may be a

continual flux of material erupting from the chamber. However, as the eruption proceeds the volatile content of the chamber may also evolve, especially if, prior to eruption, the magma in the chamber has partially degassed so that the volatile content of the magma recharging the system is greater than that in the chamber. This, in turn, may lead to an increase in the eruption rate, and possibly a transition from effusive to fire-fountaining activity. This is a complex process, since the evolution of the eruption depends on the evolution of the conduit shape and size as well as the conditions in the chamber. However, if the bubbly layer continues to erupt for some time, with an eruption rate $Q_e(t)$, then the concentration of this layer will evolve according to (cf. Eq. 16):

$$L\frac{\mathrm{d}hc}{\mathrm{d}t} = Q_b - Q_e c - Lv_s c \qquad (18)$$

where the additional term on the right-hand side denotes the loss of bubbles in the erupting mixture. Eventually, the system may evolve towards a quasi-steady state in which the volume concentration of bubbles in the chamber is $c_e = Q_b/(Q_e + Lv_s) \approx 0.1$ (Eq. 18). Although the system may not reach this steady state, it is of interest to estimate c_e and hence determine the possible bubble concentration in the chamber. Indeed, before reaching this steady-state concentration at which the bubble flux to the chamber matches the loss from the chamber, the magma eruption rate may exceed the recharge rate to the chamber, thereby leading to a complex sequence of eruption cycles. During a maintained eruption, the flux of gas escaping from the mixed layer and ponding at the top of the chamber, $\sim v_s c$ per unit area, will increase to values of order 10^{-7}–10^{-6} m/s per unit area of the chamber roof for bubbles of rise speed 10^{-6}–10^{-5} m/s. Depending on the details of the bubble size and recharge flux, this may represent a significant fraction of the recharge flux of gas. Indeed, after about 10^6–10^7 s, this foam layer might then become sufficiently deep to interrupt the eruption of the underlying bubbly magma, as envisaged by Vergniolle and Jaupart [2], leading to a period of gas-rich eruptive activity. It is also possible that some of the gas in the foam may leak from the chamber through fractures in the chamber roof and crust. Field evidence shows that volatiles issue from a wide region around the summit of Mauna Loa [1], suggesting that the crust may be quite permeable. For permeabilities K in the range 10^{-12}–10^{-14} m^2, and for a chamber of depth D below the surface, the flux of gas escaping from the chamber at pressure P may be as large as $F_g \approx (K(P-P_a)/\mu D)$ per unit area, where P_a is the atmospheric pressure. This flux has magnitude in the range 10^{-7}–10^{-9} m/s for chambers a few kilometres below the surface with pressures of order 10^8 Pa. Therefore, the gas loss rate may represent a fraction 0.01–1.0 of the supply to the foam. If the gas loss represents the majority of the flux supplied to the foam, then the eruption will continue to be dominated by eruption of the bubbly layer of magma, whereas if the crust is less permeable, then a significant foam layer may develop following onset of the eruption.

5. Discussion

We have shown that as basaltic magma chambers are recharged from relatively volatile-rich basalt, a turbulent bubble plume may develop within the chamber. This can lead to formation of a deep bubbly layer of magma. Owing to magma–bubble mixing, the original volatile content of the magma may then be very different from that in the erupting material. On eruption, the upper bubbly layer may issue from the vent leading to either fire-fountaining or passive lava flow activity depending on the bubble concentration in this layer. As the eruption proceeds, the bubble content in the chamber may increase gradually, leading to an intensification of the activity. However, at later stages in the eruption, the thin foam layer which develops above the bubbly layer of magma may deepen, leading to some more complex eruptive activity as envisaged by Vergniolle and Jaupart [2]. It may also act to supply the quiescent outgassing through the flanks of the volcano [1].

It is important to stress that the various models of eruptive activity described herein are highly simplified, and that the actual system is more complex; the modelling is designed to explore

some of controlling processes in order to build up a more detailed understanding of basaltic volcanism. Particular issues which require more detailed attention include the model of the conduit flow, including two-phase flow effects and controls on the conduit size and geometry as well as improved field data on the permeability of the country rock and chamber roof and also the shape and size of the magma sills. However, the key message of this paper is that convective mixing within the magma reservoir may lead to suspension of bubbles in the magma for some time, and this may delay the formation of the foam layer at the roof of the chamber. Depending on the relative time scales of chamber pressure build-up and foam growth, this could lead to a diverse range of eruption regimes involving either the relatively low-volatile-content bubbly magma or the highly explosive foam.

Acknowledgements

This work is supported by the Leverhulme Foundation. A.W.W. has had useful discussions with Silvana Cardoso about this project.*[AC]*

References

[1] S. Ryan, Quiescent outgassing of Mauna Loa Volcano, 1958–1994, in: Mauna Loa Revealed: Structure, Composition, History and Hazards, Am. Geophys. Union Geophys. Monogr. 92, 1990.
[2] S. Vergniolle, C. Jaupart, Dynamics of degassing at Kilauea volcano, Hawaii, J. Geophys. Res. 95 (1990) 2793–3001.
[3] F.W. Klein, R. Koyanagi, J. Nakata, W. Tanigawa, The seismicity of Kilauea's magma system, USGS Prof. Pap. 1350 (1987) 1019–1185.
[4] J. Dvorak, D. Dzurisin, Variations in magma supply rate at Kilauea volcano, Hawaii, J. Geophys. Res. 98 (1993) 22255–22268.
[5] T.M. Gerlach, E.J. Graber, Volatile budget of Kilauea volcano, Nature 313 (1985) 273–278.
[6] C. Jaupart, S. Vergniolle, Laboratory models of Hawaiian and Strombolian eruptions, Nature 331 (1988) 58–60.
[7] C. Jaupart, S. Vergniolle, The generation and collapse of a foam layer at the top of a basaltic magma chamber, J. Fluid Mech. 203 (1989) 347–380.
[8] L. Wilson, J. Head, Ascent of magma on Earth and Moon, J. Geophys. Res. 86 (1981) 2971–3001.
[9] E.A. Parfitt, L. Wilson, Explosive volcanic eruptions. IX – The transitions between Hawaiian-style lava fountaining and Strombolian activity, Geophys. J. Int. 121 (1995) 226–232.
[10] A.W. Woods, S.S.S. Cardoso, Bubble magma separation as a trigger of basaltic volcanic eruptions, Nature 385 (1997) 518–520.
[11] S.S.S. Cardoso, A.W. Woods, On convection in a volatile saturated magma, Earth Planet. Sci. Lett. 168 (1999) 301–310.
[12] S. Tait, C. Jaupart, S. Vergniolle, Pressure, gas content, and eruption periodicity of a shallow crystallising magma chamber, Earth Planet. Sci. Lett. 92 (1989) 107–123.
[13] A.W. Woods, D. Pyle, The control of magma volatile content and chamber geometry on the trigerring of volcanic eruptions, Earth Planet. Sci. Lett. 151 (1997) 155–166.
[14] J.S. Turner, Buoyancy Effects in Fluids, Cambridge University Press, Cambridge, 1979.
[15] T. Murase, A. McBirney, Properties of some common igneous rocks and their magmas at high temperature, Geol. Soc. Am. Bull. 84 (1974) 3563–3592.
[16] T. McDougall, Bubble plumes in stratified environments, J. Fluid Mech. (1978) 62–85.
[17] A. Leitch, W. Baines, Liquid volume flux in a weak bubble plume, J. Fluid Mech. 205 (1989) 77–98.
[18] C. Cashman, M. Mangan, in: Carroll, Holloway (Eds.), Volatiles in Magmas, Mineralogical Society of America, 1994.
[19] J. Moore, J. Batchelder, C. Cunningham, CO_2 filled vesicles in mid ocean basalt, J. Volcanol. Geotherm. Res. 2 (1977) 309–327.
[20] R.S.J. Sparks, The dynamics of bubble formation and growth in magmas – a review and analysis, J. Volcanol. Geotherm. Res. 3 (1978) 1–37.
[21] D.M. Pyle, D.L. Pyle, Bubble migration and the initial of volcanic eruptions, J. Volcanol. Geotherm. Res. 67 (1995) 227–232.
[22] R. Clift, J. Grace, M. Weber, Bubbles, Drops and Particles, Academic Press, London, 1978.
[23] J. Hadamard, Mouvement permanent lent d'une spheère liquide et visqueuse dans une liquide visqueax, CR Acad. Sci. 152 (1911) 1735–1738.
[24] R.S.J. Sparks, M.I. Bursik, S. Carey, L. Glaze, J. Gilbert, H. Sigurdsson, A. Woods, Volcanic Plumes, Wiley, New York, 1997.
[25] R. Kimura, Cell formation in the convective mixed layer, Fluid Dyn. Res. 3 (1987) 395–399.
[26] C. Isenberg, The Science of Soap Films and Soap Bubbles, Tieto, Clevedon, 1978, pp. 188.
[27] W.D. Baines, J. Turner, Turbulent buoyant convection from a source in a confined region, J. Fluid Mech. 37 (1969) 51–80.
[28] E.J. List, Turbulent jets and plumes, in: Fischer (Ed.),

Mixing in Coastal Waters and Estuaries, 1979, pp. 315–389.
[29] C. Jaupart, C. Allegre, Eruption rate and instabilities of eruption regime in silicic volcanoes, Earth Planet. Sci. Lett. 102 (1991) 413–429.
[30] S.M. Bower, A.W. Woods, The control of magma volatile content and chamber depth on the mass erupted during explosive volcanic eruptions, J. Geophys. Res. 102 (1997) 10273–10290.
[31] D. Martin, R. Nokes, Crystal settling in a vigorously convecting magma chamber, Nature 332 (1988) 543–546.